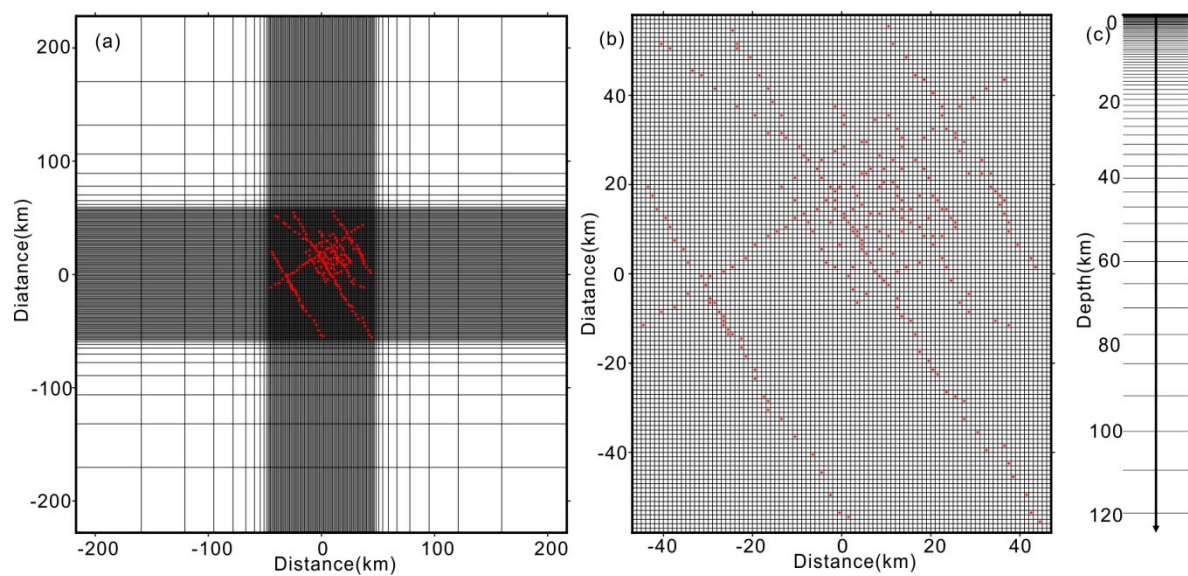
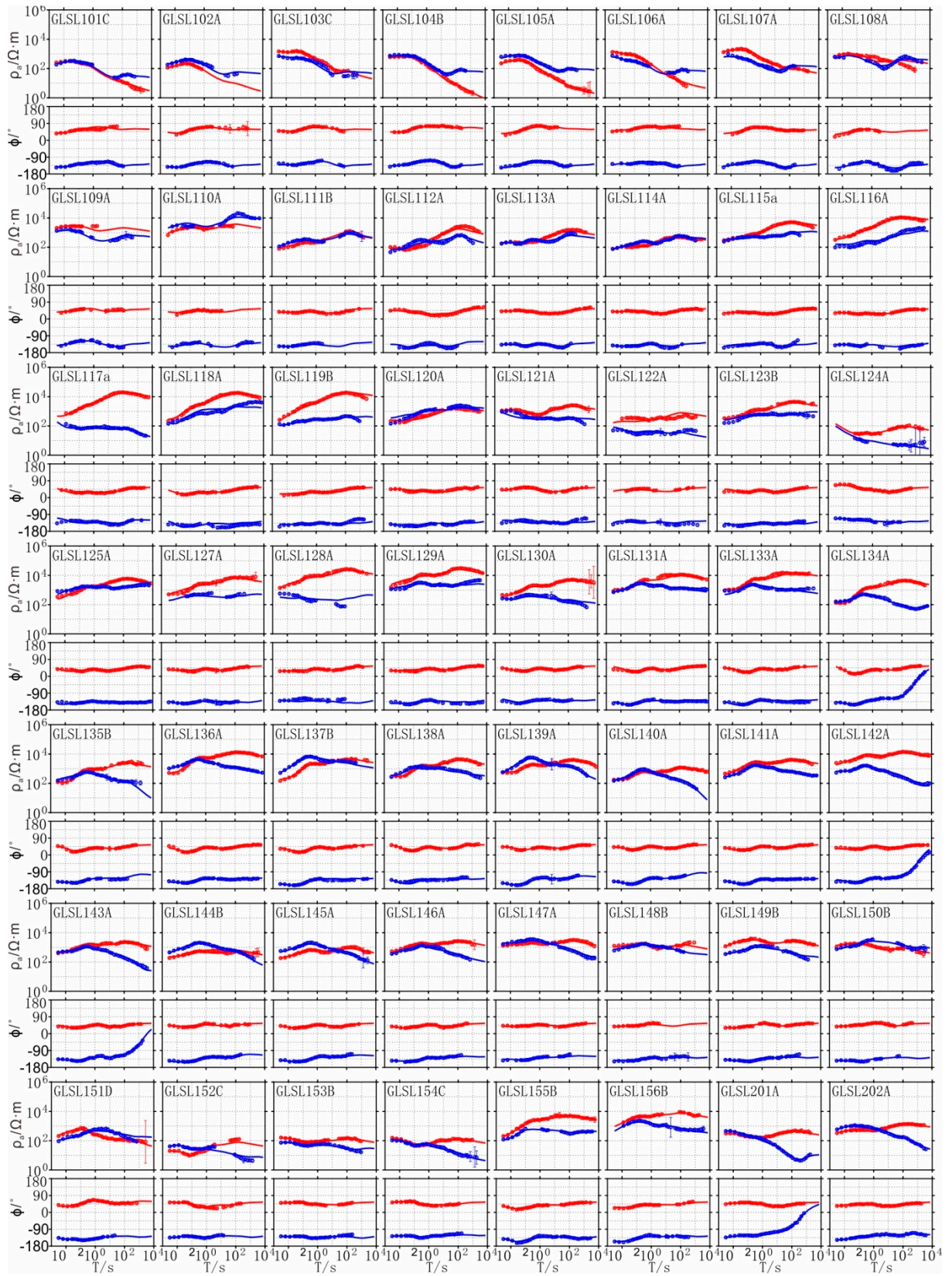


### 1. 3D inversion mesh division



**Figure S1.** (a) Horizontal grid for the 3D inversion model. (b) Central part of the horizontal grid. (c) Vertical grid within the depth of 120 km.

## 2. Fitting curves of apparent resistivity and phase for the 3D inversion



**Figure S2-1.** Observed data (points with error bar) and response data (line) of the 3D inversion. Red line and points denote XY components; Blue line and points denote YX components.



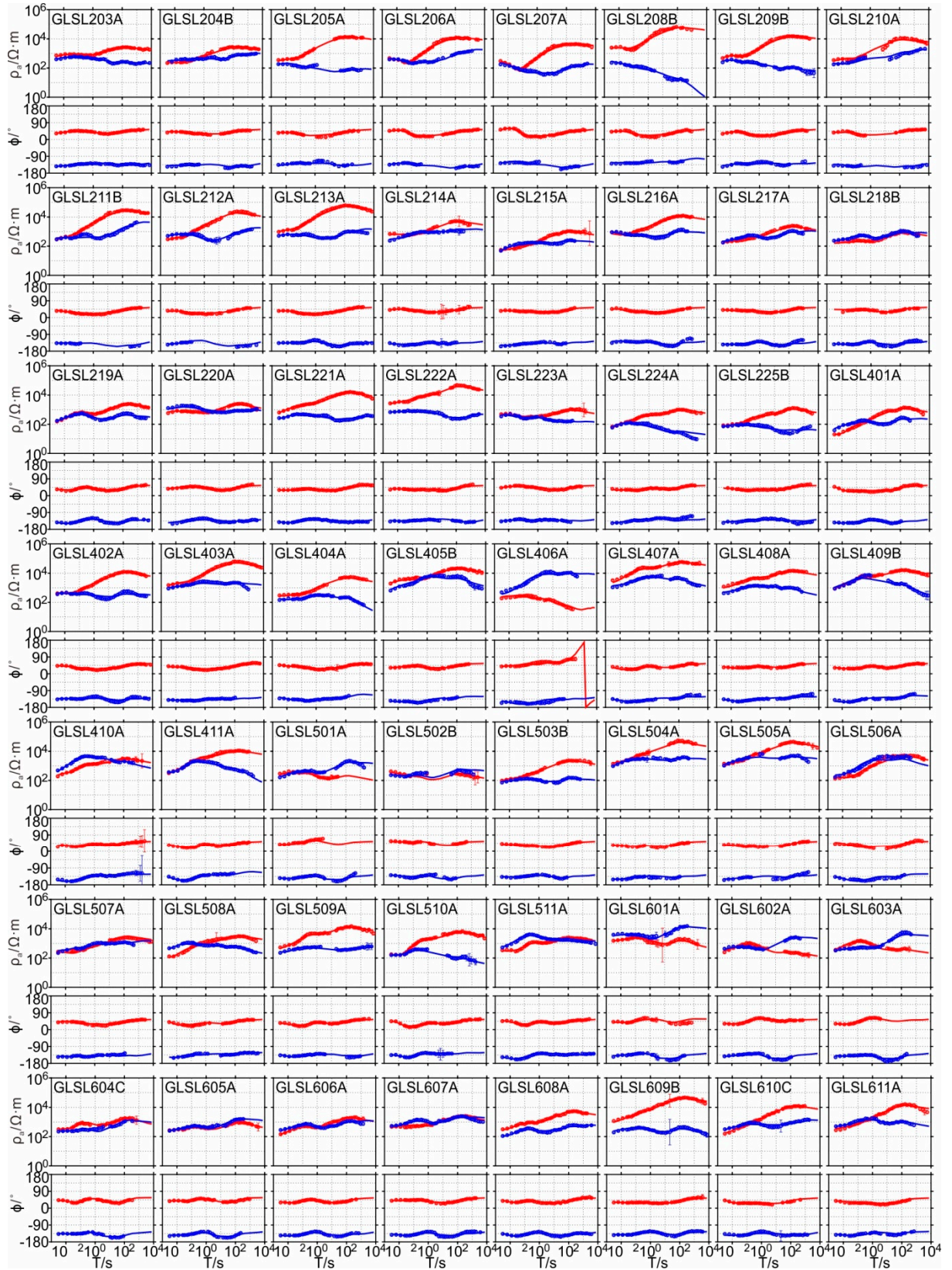


**Figure S2-2.** Observed data (points with error bar) and response data (line) of the 3D inversion. Red line and points denote XY components; Blue line and points denote YX components.



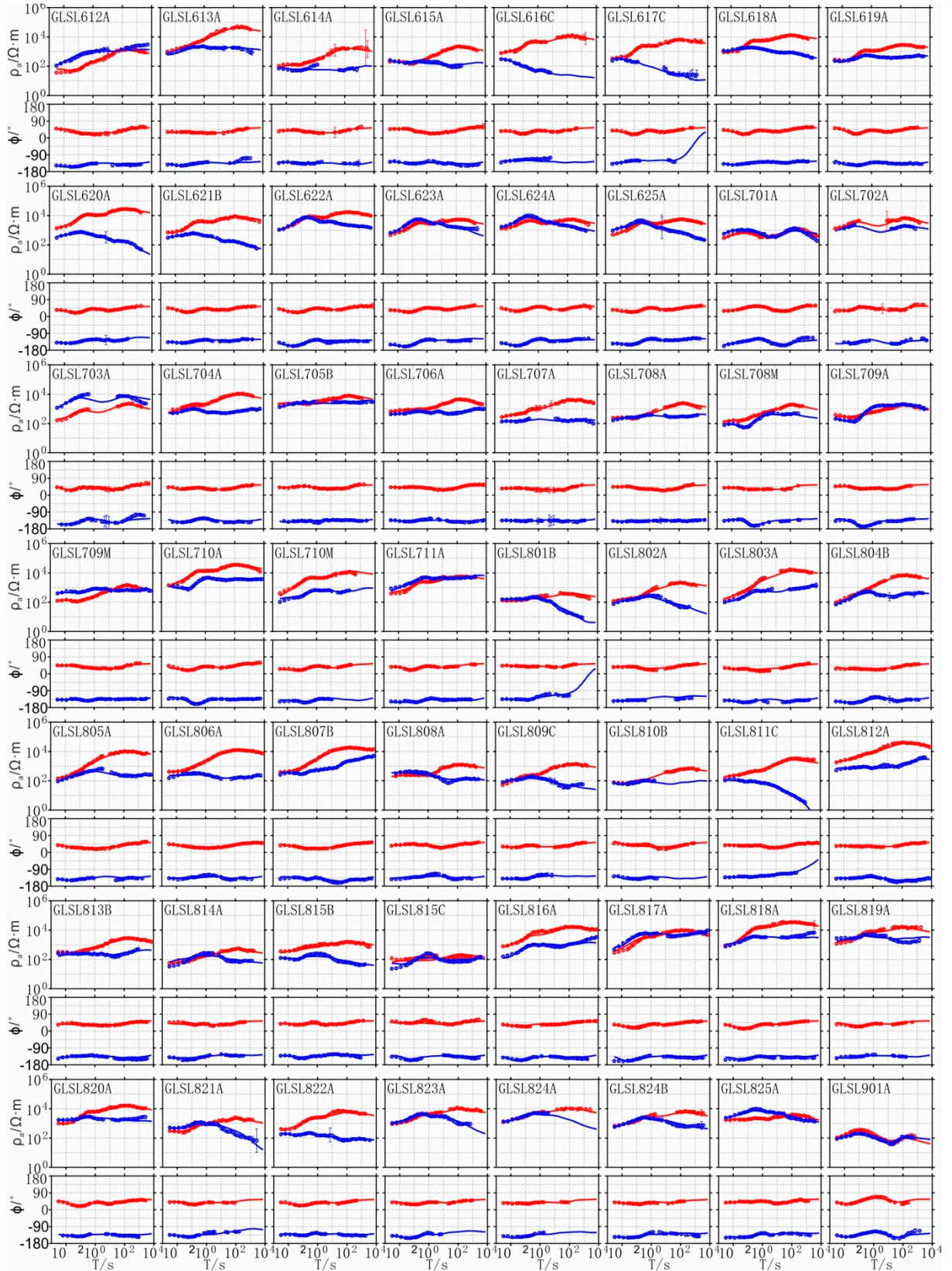


**Figure S2-3.** Observed data (points with error bar) and response data (line) of the 3D inversion. Red line and points denote XY components; Blue line and points denote YX components.



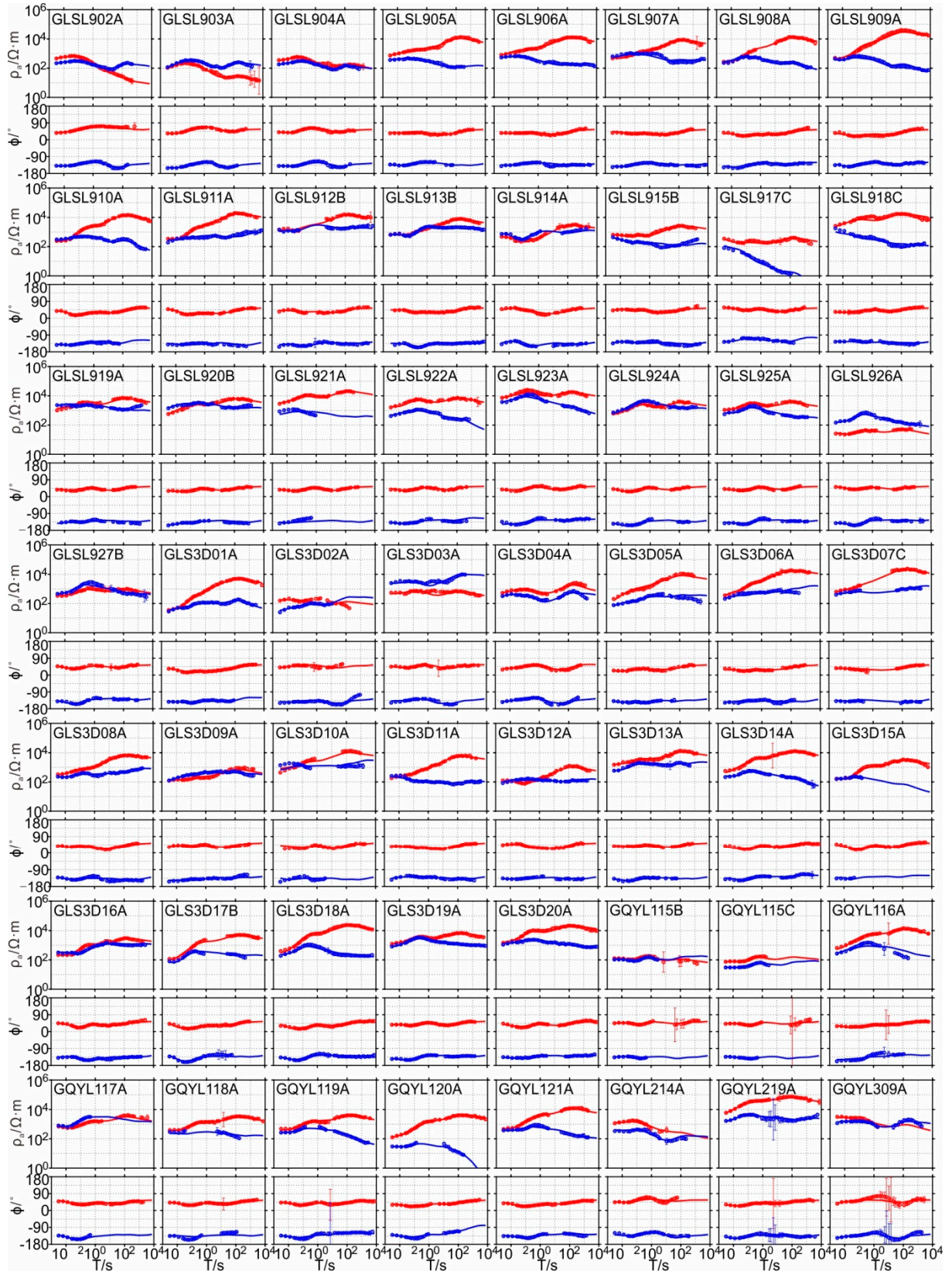


**Figure S2-4.** Observed data (points with error bar) and response data (line) of the 3D inversion. Red line and points denote XY components; Blue line and points denote YX components.

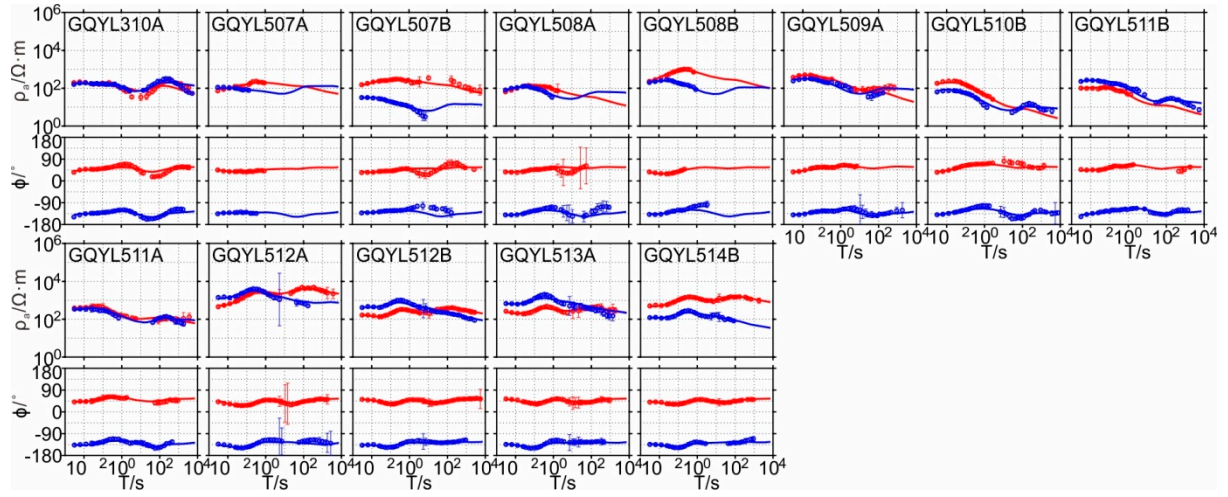


**Figure S2-5.** Observed data (points with error bar) and response data (line) of the 3D inversion. Red line and points denote XY components; Blue line and points denote YX components.



### 3. Resistivity Structure Model Sensitivity Testing

Figure S3 reveals the deep resistivity structures for four profiles that trend in a northwest-southeast direction and one profile that trends in a southwest-northeast direction. These structures were obtained through 3D inversion.

To assess the dependability of the resistivity structure derived from the inversion, sensitivity tests were carried out on the effective depth and crucial structural sections. The fitting variation characteristics were described using the RMS update:

$$\text{RMS update} = \frac{RMS_{\text{new}} - RMS_{\text{origin}}}{RMS_{\text{origin}}} \times 100\%$$

RMS update reflects the change in root mean square error that occurs when the model is modified.  $RMS_{\text{new}}$  and  $RMS_{\text{origin}}$  represent the root mean square errors for the modified and inversion models, respectively. If the RMS update is positive, it means that the modification made the fit worse. On the other hand, a negative value indicates that the fit has improved.

Firstly, sensitivity testing was conducted on the detection depth. Resistivity values below 10 km, 20 km, and 30 km in the resistivity structure model were modified to the initial model resistivity value (500  $\Omega\text{m}$ ) for forward modeling. The resulting  $RMS_{\text{new}}$  and RMS update distribution maps are shown in Figure S4. Figures S4b-d indicate that the modified models below 10 km and 20 km depth had  $RMS_{\text{new}}$  values greater than 5 at numerous measurement points in the Lingshan seismic zone, whereas the  $RMS_{\text{new}}$  values at 30 km depth approached 3. Figures S4e-g show that all RMS update values are positive, indicating that the fit deteriorated, particularly in the Lingshan seismic zone. It appears that the models resulting from the inversion are limited by the available data up to a depth of 30 km in the Lingshan seismic zone. Nevertheless, in the northwest section of the survey area, certain measurement points indicate only slight variations in  $RMS_{\text{new}}$ . This is probably because of the protective influence of the low-resistivity layers (Figure 8) found in the middle to the shallow crust, which leads to a shallower detection depth in that particular region.

Secondly, sensitivity testing was conducted on specific structural sections. A forward modeling analysis was conducted on the low-resistivity structure C3 and the high-resistivity structure R1 below the Lingshan seismic zone (Figure 8 and S3). Modifying the resistivity values of C3 in the depth range of 4-10 km to 5000  $\Omega\text{m}$  for forward modeling yielded RMS update distributions shown in Figure S5a, where some measurement points around C3 reached up to 50%. The forward modeling findings for R1, using resistivity values of 500, 1000, and 10000  $\Omega\text{m}$  throughout the depth range of 4-10 km, revealed that changes to resistivity values of 500 and 1000  $\Omega\text{m}$  led to a considerable decrease in the accuracy of the fit around R1. However, alterations to the resistivity value of 10000  $\Omega\text{m}$  resulted in only slight improvements in the RMS update. The forward modeling results indicate that the low-resistivity structure C3 and the high-resistivity structure R1 obtained in the Lingshan seismic zone are reliable.

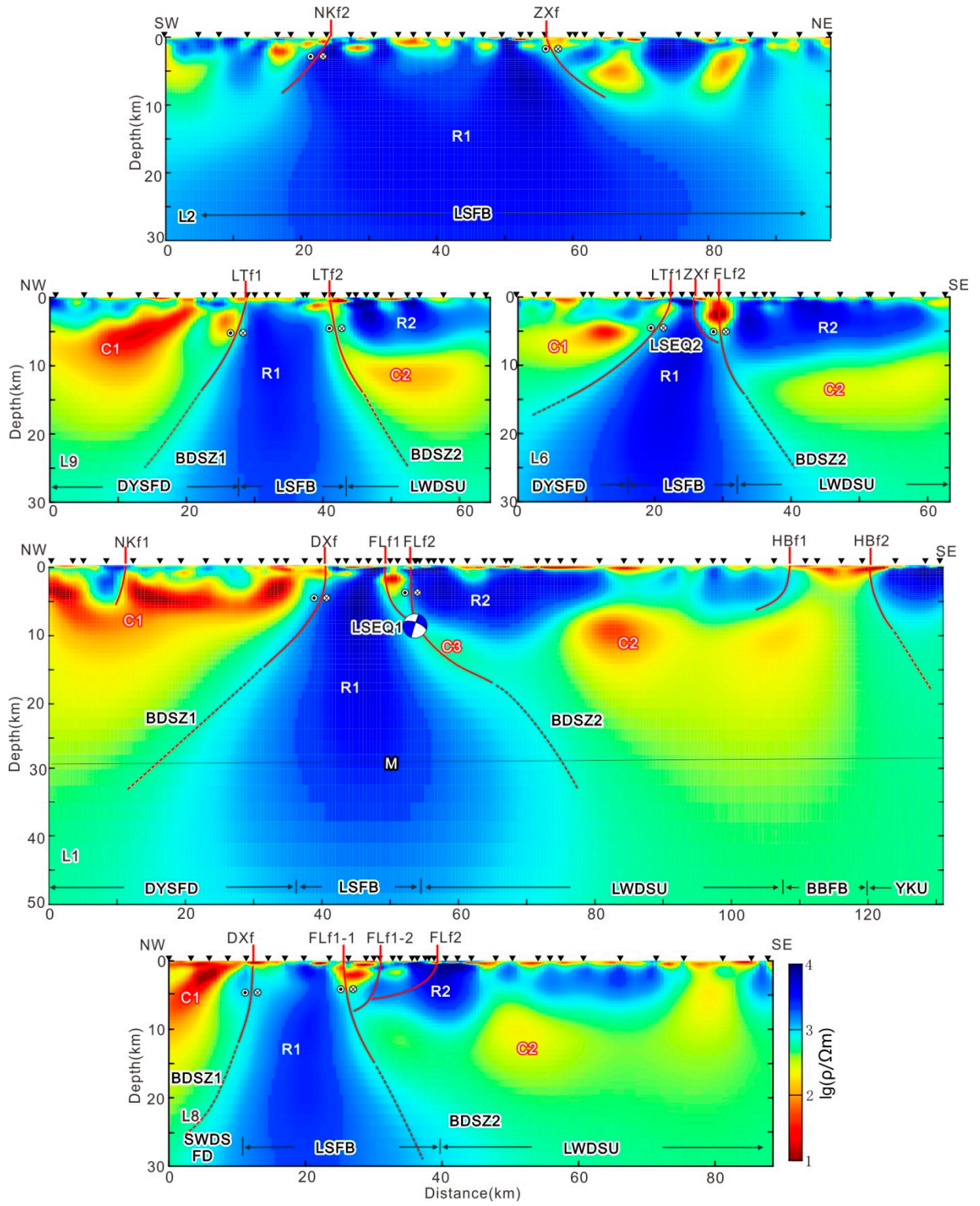


**Figure S3.** presents the deep resistivity structures for four NW-SE trending profiles and one SW-NE trending profile obtained through 3D inversion. (see Figure 2 for the locations of cross sections). The names of construction unit and faults are consistent with those in Figures 1 and 2.



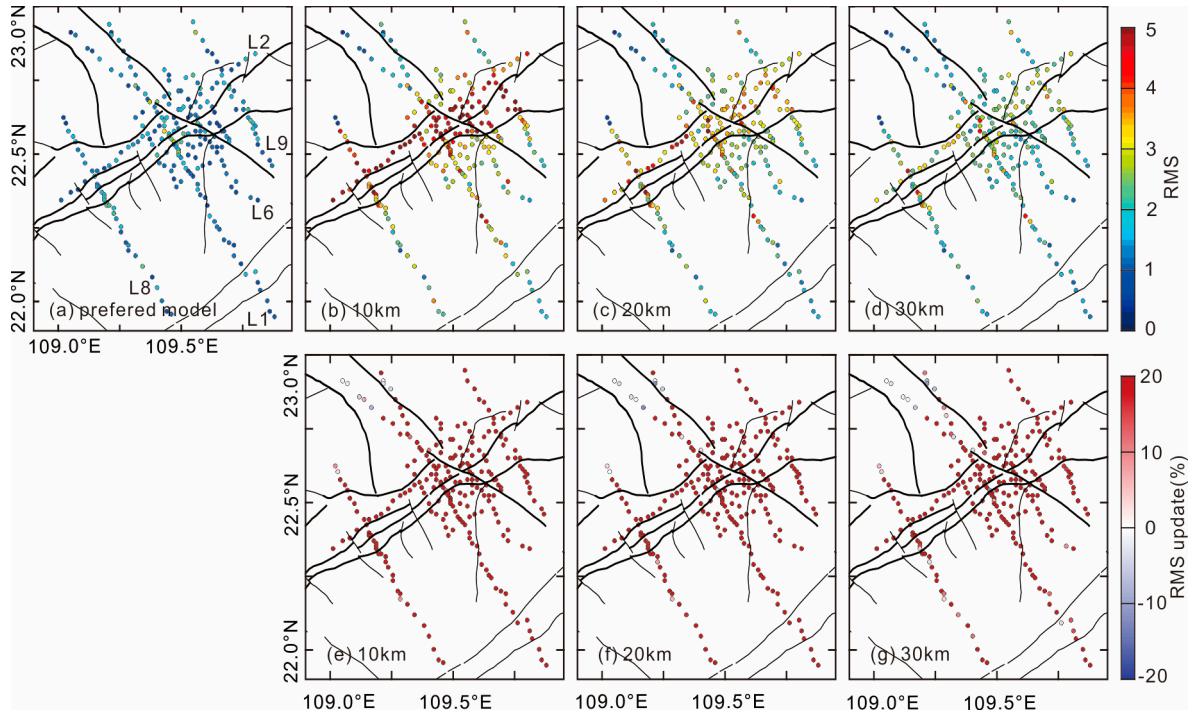


**Figure S4.** RMS distribution map of resistivity structure model sensitivity testing about the detection depth. (a) Distribution map of  $RMS_{origin}$ . (b), (c), (d)  $RMS_{new}$  of the forward models below 10 km and 20 km depth, respectively. (e), (f), (g) RMS update of the modified models below 10 km and 20 km depth, respectively.

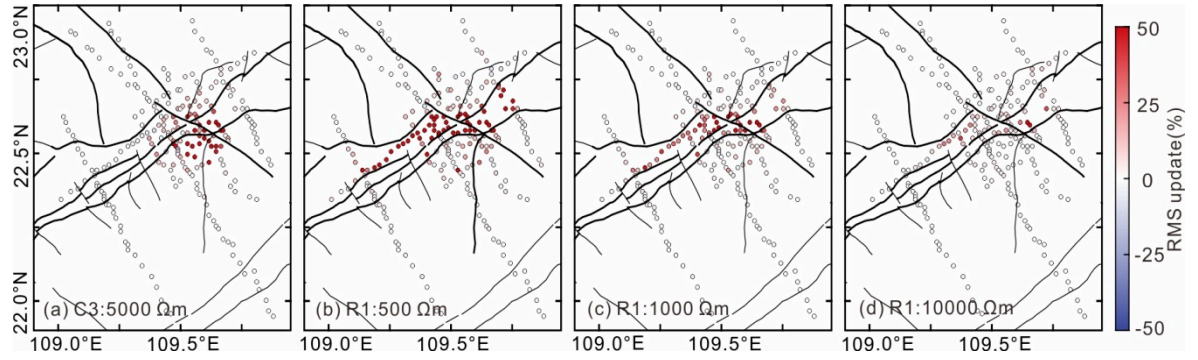


**Figure S5.** RMS update of C3 and R1 in Lingshan seismic zone.